Cell Wall Modifications in Arabidopsis Plants with Altered α-L-Arabinofuranosidase Activity[C][W]

Ricardo A. Chávez Montes, Philippe Ranocha, Yves Martinez, Zoran Minic[1], Lise Jouanin, Mélanie Marquis, Luc Saulnier, Lynette M. Fulton[2], Christopher S. Cobbett, Frédérique Bitton, Jean-Pierre Renou, Alain Jauneau, and Deborah Goffner*

UMR 5546, CNRS-Université Paul Sabatier, Surfaces Cellulaires et Signalisation chez les Végétaux, BP 42617 Auzeville, 31326 Castanet-Tolosan, France (R.A.C.M., P.R., Y.M., A.J., D.G.); Laboratoire de Biologie Cellulaire, Institut National de la Recherche Agronomique, 78026 Versailles cedex, France (Z.M., L.J.); Biopolymères Interactions Assemblages, Unité de Recherche sur les Polysaccharides leurs Organisations et Interactions, Institut National de la Recherche Agronomique, BP 71627, 44316 Nantes cedex 03, France (M.M., L.S.); Department of Genetics, University of Melbourne, Victoria 3010, Australia (L.M.F., C.S.C.); and Unité de Recherche en Génomique Végétale, INRA-CNRS, CP 5708, 91057 Evry cedex, France (F.B., J.-P.R.)

Although cell wall remodeling is an essential feature of plant growth and development, the underlying molecular mechanisms are poorly understood. This work describes the characterization of Arabidopsis (*Arabidopsis thaliana*) plants with altered expression of ARAF1, a bifunctional α-L-arabinofuranosidase/β-D-xylosidase (At3g10740) belonging to family 51 glycosyl-hydrolases. *ARAF1* was localized in several cell types in the vascular system of roots and stems, including xylem vessels and parenchyma cells surrounding the vessels, the cambium, and the phloem. *araf1* T-DNA insertional mutants showed no visible phenotype, whereas transgenic plants that overexpressed ARAF1 exhibited a delay in inflorescence emergence and altered stem architecture. Although global monosaccharide analysis indicated only slight differences in cell wall composition in both mutant and overexpressing lines, immunolocalization experiments using anti-arabinan (LM6) and anti-xylan (LM10) antibodies indicated cell type-specific alterations in cell wall structure. In *araf1* mutants, an increase in LM6 signal intensity was observed in the phloem, cambium, and xylem parenchyma in stems and roots, largely coinciding with *ARAF1* expression sites. The ectopic overexpression of ARAF1 resulted in an increase in LM10 labeling in the secondary walls of interfascicular fibers and xylem vessels. The combined *ARAF1* gene expression and immunolocalization studies suggest that arabinan-containing pectins are potential in vivo substrates of ARAF1 in Arabidopsis.

Cell walls undergo dynamic changes during plant growth and development. Wall composition and macromolecular assembly vary greatly among taxa, species, organs, and cell types within an individual or domains of a given cell wall. These differences contribute to cell shape and, in some cases, specialized cellular function. Cell wall-related genomic approaches in different physiological contexts have revealed that many cell wall biosynthetic/modifying enzymes and structural proteins are regulated at the transcriptional level. In the case of secondary wall formation, one can correlate morphological and cytological cellular changes with the spatial and temporal regulation of wall-modifying enzymes over a developmental xylem gradient in poplar (*Populus* spp.; Schrader et al., 2004) and in in vitro tracheary elements (TEs) of zinnia (*Zinnia elegans*; Milioni et al., 2001; Demura et al., 2002; Pesquet et al., 2005). In a genomic approach of zinnia TEs, Pesquet et al. (2005) identified a family 51 (Carbohydrate Active enZYmes [CAZY] database, http://www.cazy.org; Coutinho and Henrissat, 1999) α-L-arabinofuranosidase (arabinofuranosidase) that was highly expressed in TE induction medium at the onset of secondary wall formation. Interestingly, although relatively little redundancy was observed in sequence data generated from the different genomic studies in zinnia, this family 51 arabinofuranosidase gene was systematically identified. At3g10740 is the closest Arabidopsis (*Arabidopsis thaliana*) homolog to the arabinofuranosidase zinnia sequence identified. Although At3g10740 was originally named *ASD1*, we refer to it as *ARAF1* from here on, because ARAf was the name attributed to the corresponding purified protein (Minic et al., 2004). This enzyme belongs to family 51 glycosyl-hydrolases (GHs), but similar enzymatic activities are found for enzymes that belong to family 3 GHs.

α-L-Arabinofuranosidases (EC 3.2.1.55) are defined as enzymes that catalyze the hydrolysis of terminal nonreducing α-L-arabinofuranoside residues. However,

[1] Present address: Department of Chemistry, University of Saskatchewan, 110 Science Place, Saskatoon, SK S7N 5C9, Canada.

[2] Present address: Entwicklungsbiologie der Pflanzen, Wissenschaftszentrum Weihenstephan, Technische Universität Munich, Am Hochanger 4, D–85354 Freising, Germany.

* Corresponding author; e-mail goffner@scsv.ups-tlse.fr.

The author responsible for distribution of materials integral to the findings presented in this article in accordance with the policy described in the Instructions for Authors (www.plantphysiol.org) is: Deborah Goffner (goffner@scsv.ups-tlse.fr).

[C] Some figures in this article are displayed in color online but in black and white in the print edition.

[W] The online version of this article contains Web-only data.

www.plantphysiol.org/cgi/doi/10.1104/pp.107.110023

several enzymes in families 3 and 51 are capable of hydrolyzing both L-Ara and D-Xyl from a variety of substrates in vitro and therefore may be considered as bifunctional arabinofuranosidase/β-D-xylosidase (xylosidase; EC 3.2.1.37) enzymes. For example, when considering barley (*Hordeum vulgare*) ARA-I, Arabidopsis XYL3 and ARAF1, and alfalfa (*Medicago sativa*) MsXyl1, the k_{cat}/K_m ratio using artificial substrates such as 4-nitrophenyl-α-L-arabinofuranose (pNPA) and 4-nitrophenyl-β-D-xylopyranose are of the same order of magnitude, suggesting that they are true bifunctional enzymes (Lee et al., 2003; Minic et al., 2004, 2006; Xiong et al., 2007). The hydrolytic activity of many of these enzymes has also been tested with natural polysaccharidic substrates. For example, barley ARA-I preferentially hydrolyzes D-Xyl rather than L-Ara residues of wheat (*Triticum aestivum*) arabinoxylan (WAX; Lee et al., 2003), whereas XYL3 and ARAF1 from Arabidopsis and MsXyl1 from alfalfa hydrolyze both L-Ara and D-Xyl from WAX and L-Ara from sugar beet (*Beta vulgaris*) arabinan (SBA) at approximately the same rates in vitro (Minic et al., 2004, 2006; Xiong et al., 2007). In contrast, barley XYL hydrolyzes only D-Xyl from WAX and has a k_{cat}/K_m ratio for 4-nitrophenyl-β-D-xylopyranose approximately 30-fold higher than for pNPA, suggesting that it is a true xylosidase (Lee et al., 2003). The barley AXAH-I hydrolyzes L-Ara from SBA, larchwood (*Larix dahurica*) arabinogalactan, and WAX, but not D-Xyl from WAX, suggesting that it is more likely true arabinofuranosidase (Lee et al., 2001). Although biochemical data for purified radish (*Raphanus sativus*) RsAraf1 are not available, its overexpression in Arabidopsis provoked an increase in total arabinofuranosidase activity with only a minor increase in total xylosidase activity, suggesting that it is also a true arabinofuranosidase (Kotake et al., 2006). Finally, Japanese pear (*Pyrus pyrifolia*) PpARF2 hydrolyzes L-Ara from SBA but does not hydrolyze L-Ara or D-Xyl from WAX, indicating that it is a pectin-specific true arabinofuranosidase (Tateishi et al., 2005). Because enzymatic activity does not necessarily correlate with the protein primary structure, the plant gene database annotations "α-L-arabinofuranosidase" and "β-D-xylosidase" should be regarded with skepticism until biochemical and physiological data become available.

At the molecular level, *ARAF1* gene expression and that of another closely related family 51 arabinofuranosidase gene, At5g26120 (*ARAF2*), have been partially characterized in Arabidopsis (Fulton and Cobbett, 2003). Whereas *ARAF2* expression was limited to the vasculature in older root tissue and in floral organs and abscission zones, *ARAF1* was expressed ubiquitously throughout the plant, and especially in vascular tissues, in agreement with data available in the Genevestigator database (https://www.genevestigator.ethz.ch/; Zimmermann et al., 2004). The deduced ARAF1 protein sequence contains an N-terminal signal peptide that predicts an extracellular localization. Moreover, proteomic analyses undertaken in Arabidopsis indicated that ARAF1 is present in the extracellular fraction (Charmont et al., 2005; Jamet et al., 2006; Minic et al., 2007). Together, these results suggest that ARAF1 acts on polysaccharides at the cell wall.

Here, we have adopted a genetic approach to determine which of the L-Ara-containing (or D-Xyl-containing) cell wall components may be the physiological substrate of ARAF1 in planta. We identified T-DNA-tagged insertional mutants lacking ARAF1 activity and produced transgenic Arabidopsis plants that overexpress ARAF1. Beyond global sugar analysis, we probed for wall modifications at the cellular level by comparing immunolocalization patterns using antibodies raised against α-(1,5)-linked L-Ara (LM6) and β-(1,4)-linked D-Xyl (LM10 and LM11) residues. The data presented suggest that arabinans are potential in vivo substrates of ARAF1.

RESULTS

pARAF1::*GUS* Analysis Revealed New Cell-Specific Expression Sites

Reverse transcription (RT)-PCR expression analysis previously indicated that *ARAF1* transcript was detected in all organs examined (Fulton and Cobbett, 2003). Data retrieved from the Genevestigator database and RT-PCR analysis carried out herein confirmed these results (https://www.genevestigator.ethz.ch/; Zimmermann et al., 2004; data not shown). To provide a comprehensive view of *ARAF1* expression, the *pARAF1*::*GUS* transformants originally described by Fulton and Cobbett (2003) were used. Fulton and Cobbett (2003) originally showed that *ARAF1* is preferentially expressed in the vascular tissues of different organs. Therefore, we undertook a detailed analysis, particularly in stems and roots, of the precise cell types expressing *ARAF1*. In 7-d-old seedlings, GUS expression was observed in the vascular cylinders of hypocotyls and roots (Fig. 1, A and B), in emerging lateral roots (Fig. 1B), and in the vasculature of cotyledons (data not shown). In the apical portion of the stem, GUS expression was localized in the phloem, cambial region, and cells surrounding the protoxylem and developing metaxylem (Fig. 1C). In the basal portion of the stem, GUS expression was identical to that in the apical portion (Fig. 1D). It is interesting that *ARAF1* was not expressed in the secondary xylem (Fig. 1D). In roots of adult plants, GUS expression was detected in the primary xylem, in patches throughout extraxylary tissues (Fig. 1E), and in developing secondary xylem vessels close to the cambium (Fig. 1F). In roots with xylem fibers, GUS activity was also present in the cambial region (Fig. 1G). Finally, GUS expression was observed in the guard cells in stems (Fig. 1H).

T-DNA-Tagged *ARAF1* Mutants Were Identified

araf1-1, a mutant line in the ecotype Wassilewskija (Ws) background, was identified in the Versailles T-DNA insertional mutant collection (Bechtold et al.,

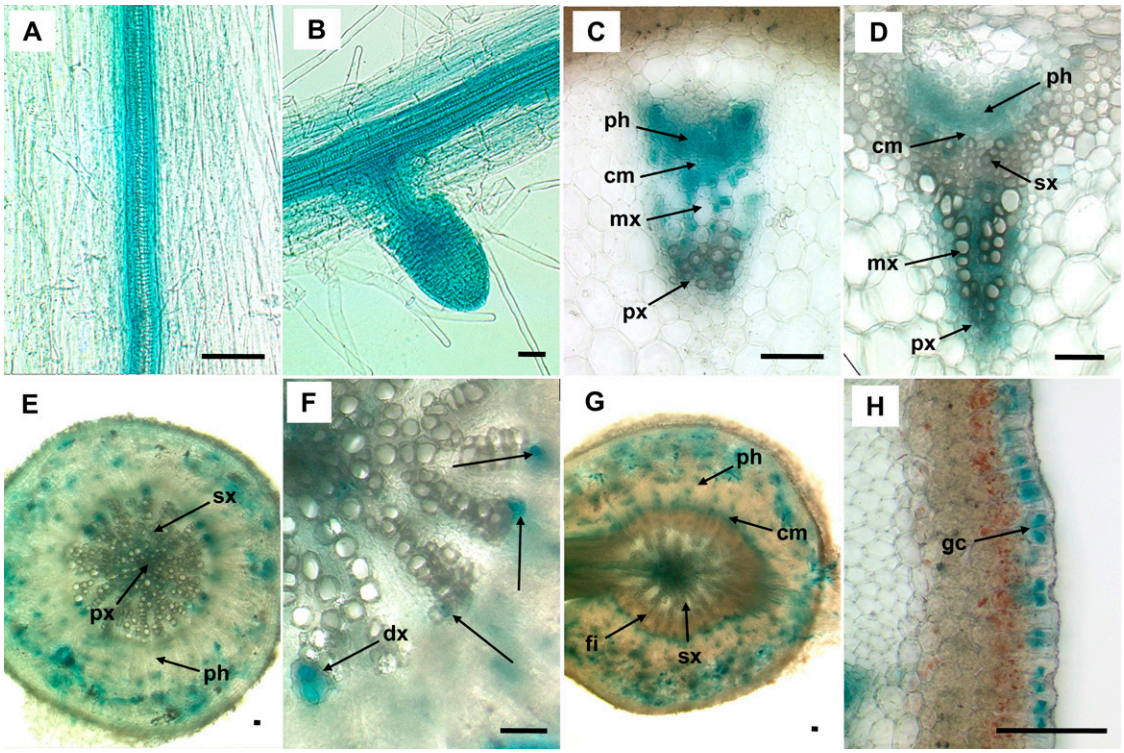

Figure 1. Histochemical localization of GUS activity in *pARAF1*::*GUS* transformants. In 7-d-old seedlings, GUS activity is visible in the vascular cylinder of the hypocotyl (A) and in root and emerging lateral roots (B). In the upper (C) and lower (D) parts of the stem, GUS activity is found in the cambium, phloem, and parenchyma cells surrounding the protoxylem and metaxylem. No activity was detected in secondary xylem. In roots of adult plants (E–G), GUS activity is present in primary xylem and extraxylary tissues (E and G) and in developing secondary xylem vessels (F). In roots with xylem fibers (G), GUS activity was also present in the cambium. GUS activity was also observed in guard cells of the stem (H). Stem cross sections were stained with phloroglucinol to reveal lignified tissues (brownish cell walls in C and D). cm, Cambium; dx, developing secondary xylem vessel; fi, fiber; gc, guard cell; mx, metaxylem; ph, phloem; px, protoxylem; sx, secondary xylem. Bars represent 50 μm.

1993). Segregation analysis on selective medium containing kanamycin and Southern-blot analysis indicated that *araf1-1* contained only one T-DNA insertion (data not shown). Sequencing confirmed that the T-DNA insertion was located in the 17th exon (Fig. 2A). No *ARAF1* transcript could be detected by RT-PCR in the *araf1-1* mutant using the rt-araf1-1 primers (Fig. 2B). However, the presence of a hybrid *ARAF1-T-DNA* mRNA transcript in the *araf1-1* mutant was detected using a gene-specific primer, hyb-araf1-1, and T-DNA right border primer, RBver (Fig. 2A; data not shown). As this could have led to the translation of a modified, yet active, form of ARAF1, wild-type and *araf1-1* stem crude protein extracts were analyzed. The arabinofuranosidase activity profiles following CM-Sepharose chromatography were obtained (Fig. 2C). From fractions 1 to 45, wild-type stems exhibited three arabinofuranosidase peaks (peaks I, II, and III), whereas *araf1-1* stems exhibited only two peaks (peaks I and III). Peak III in fractions 35 to 45 corresponded to XYL1, a previously identified and characterized bifunctional arabinofuranosdase/xylosidase (Minic et al., 2004). Fractions 10 to 20 showed two arabinofuranosidase activity peaks for the wild-type line and one in the mutant line. Peak II, which was absent in the mutant line, corresponded to ARAF1. In addition, this elution position was similar to that of previously analyzed ARAF1 (Minic et al., 2004). Peak I corresponded to ARAF2, encoded by the At5g26120 gene (Z. Minic and L. Jouanin, unpublished data). A second *araf1* mutant, *araf1-2*, a mutant in the ecotype Columbia 0 (Col0) background from the GABI-Kat collection (Rosso et al., 2003), was also identified. The available flanking sequence tag from the GABI-Kat database indicates that the T-DNA insertion in *araf1-2* was located in the 11th intron. No *ARAF1* transcript could be detected in this mutant using the hmz-araf1-2-F and rt-araf1-2-R primers (Fig. 2B).

When grown under different conditions, including in soil or in vitro, in the greenhouse or in growth chambers, *araf1-1* and *araf1-2* showed no reproducible developmental phenotype. Germination was not affected by the mutation. Because *ARAF1* was expressed in guard cells, stomatal function measurements according to Jones et al. (2003) were performed. No alterations in guard cell function could be detected as a result of the *ARAF1* mutation (S. McQueen-Mason, unpublished data).

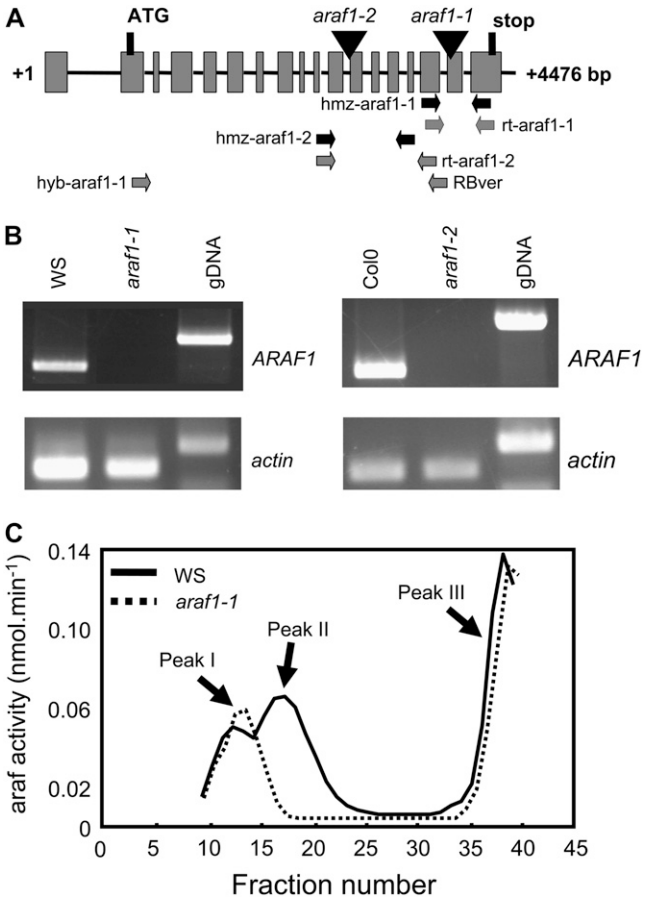

Figure 2. Schematic illustration of the intron-exon structure of the α-L-arabinofuranosidase At3g10740 gene, RT-PCR analysis of the *ARAF1* transcript in wild-type and mutant lines, and chromatographic analysis of arabinofuranosidase enzyme activities. A, Positions of the start and stop codons, T-DNA insertion in the *araf1-1* and *araf1-2* mutants (triangles), primers for PCR screening (for *araf1-1*, hmz-araf1-1; for *araf1-2*, hmz-araf1-2; black arrows), and primers for RT-PCR analysis (for *araf1-1*, rt-araf1-1, hyb-araf1-1, and RBver; for *araf1-2*, hmz-araf1-2-F and rt-araf1-2-R; gray arrows) are indicated. Primer sequences are provided in "Materials and Methods." B, RT-PCR analysis of the wild type and *araf1* mutants. Genomic DNA (gDNA) is shown as a control. C, Chromatographic analysis of arabinofuranosidase activities in Ws (continuous line) and *araf1-1* (dotted line) stems. Arabinofuranosidase activities were fractionated by cation-exchange chromatography.

35S::*ARAF1* Transgenic Lines Exhibited Developmental Stem Phenotypes

To generate ARAF1-overexpressing lines, Col0 plants were transformed with a 35S::ARAF1 construct. Homozygous transformant seedlings were screened by semiquantitative RT-PCR for increased ARAF1 transcript accumulation, and three independent lines, 35S::ARAF1a, 35S::ARAF1b, and 35S::ARAF1c, were selected (Fig. 3A). Activity assays performed on total protein extracts of adult stems using pNPA as a substrate indicated an 8-fold increase in total arabinofuranosidase activity in the 35S::ARAF1a line and a 25-fold increase in the 35S::ARAF1b and 35S::ARAF1c lines compared with Col0 plants (Fig. 3B). Many developmental parameters, including germination, stem elongation rate, silique development, and seed yield, were unchanged in all 35S::ARAF1 lines. However, detailed observation showed that the three lines exhibited a delay in inflorescence emergence (growth stage 5.10; Boyes et al., 2001) of approximately 1 week (Fig. 4A).

Arabidopsis plants have a nonuniform number of secondary stems (defined as stems emerging from the main stem). Under our standard growth conditions, the majority of individuals in a wild-type population had n secondary stems. The value for n varied among experiments (between 3 and 5). *35S::ARAF1* populations exhibited an altered distribution in the number of secondary stems, with the majority of plants having $n - 1$ secondary stems (Fig. 4C). A representative experiment is shown in Figure 4B. The majority of wild-type Col0 plants (63%) had an average of three secondary stems, with fewer than 20% of the individuals having either two or four secondary stems. In contrast, nearly 80% of the *35S::ARAF1a* and *35S::ARAF1b* individuals had only two secondary stems, and plants with four secondary stems were absent in *35S::ARAF1a* and *35S::ARAF1b* populations.

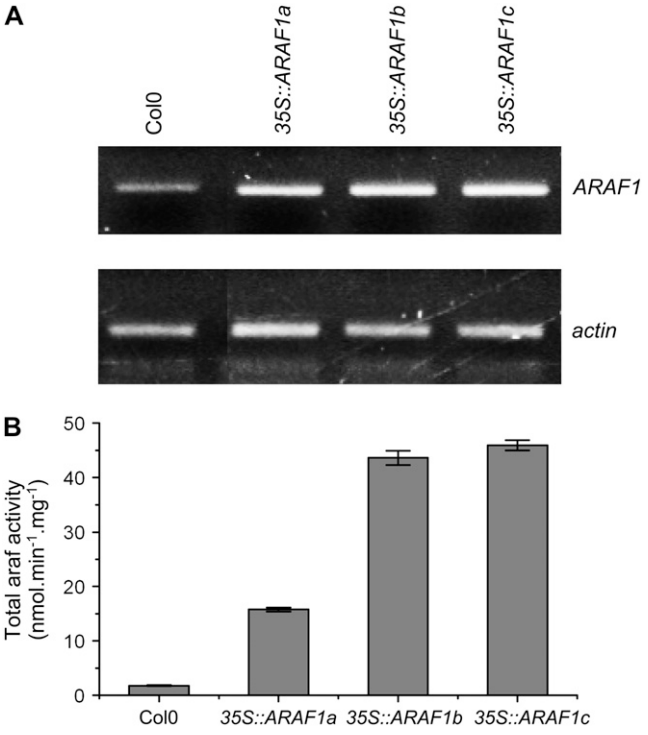

Figure 3. Semiquantitative RT-PCR analysis and total arabinofuranosidase activity in crude stem extracts of three independent ARAF1-overexpressing lines. A, Semiquantitative RT-PCR analysis of *ARAF1* transcript levels in 7-d-old seedlings of the wild type (Col0) and three independent homozygous *35S::ARAF1* lines. Actin amplification is shown as a control. B, Total arabinofuranosidase activity using 4-nitrophenyl-α-L-arabinofuranose as substrate in crude extracts of the lower part of the stem. Error bars indicate SD.

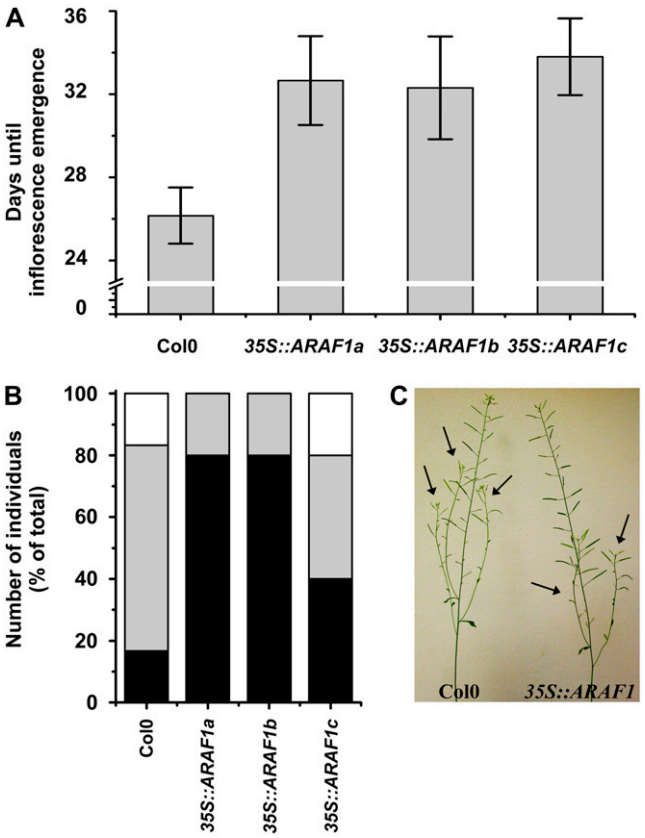

Figure 4. Developmental phenotypes in ARAF1-overexpressing lines. A, Number of days after imbibition required for inflorescence emergence (as defined by Boyes et al. [2001]) in Col0 and *35S::ARAF1* transformants. $n = 20$ per line. Error bars represent SD. B, Representative experiment showing the number of individuals with two (black bars), three (gray bars), or four (white bars) secondary stems in Col0 and *35S::ARAF1* transformants. $n = 12$ per line. C, Col0 and *35S::ARAF1* transformants with three and two secondary stems, respectively. [See online article for color version of this figure.]

Modification of ARAF1 Activity in Planta Revealed Subtle Changes in Global Monosaccharide Composition

As a first step in assessing the role of ARAF1 in dictating cell wall polysaccharide composition, we determined the repercussions of the absence or overexpression of ARAF1 on the monosaccharide content of alcohol-insoluble residue (AIR) from the wild type, the *araf1-1* mutant, and *35S::ARAF1* transformants (Table I). Dry seeds, roots, and the upper and lower portions of the stem were all examined because of the ubiquitous expression of ARAF1. In general, L-Ara content was high in seeds (16 mol %) compared with the other organs studied (1–5 mol %). Minor yet significant differences in the amount of some sugars were observed. For example, in dry seeds, L-Ara content was higher in the *araf1-1* mutant and lower in *35S::ARAF1* transformants. In roots and the basal portion of the stem, D-Xyl content was significantly higher in *35S::ARAF1* lines than in Col0. However, no differences in D-Xyl content were observed for the *araf1-1* mutant. Uronic acid content was also significantly lower in the *35S::ARAF1* lines compared with Col0 in the basal portion of the stem.

Immunolocalization Studies Point to Cell Type-Specific Modifications of Cell Wall Polysaccharides in Plants with Modified ARAF1 Activity

Because changes in *ARAF1* gene expression had only a limited impact on the global monosaccharide composition of the cell wall, we undertook a more detailed analysis of the cell wall by immunolocalization using antibodies raised against specific polysaccharidic wall structures. These studies provide clues to identify in vivo enzyme substrates at the cellular level, even those too subtle to detect by global analyses. Based on in vitro biochemical data for ARAF1, we first compared LM6 epitope distribution in wild-type, mutant, and overexpressing lines. LM6 recognizes arabinans found in pectin and some proteins (Willats et al., 1998; Lee et al., 2005; Harholt et al., 2006). The observations described below for *araf1-1* were confirmed with the *araf1-2* mutant (data not shown).

The distribution of LM6 epitopes was first investigated in the basal portions of the stem. In the wild type, relatively intense labeling was found in the epidermal cell walls, with very weak labeling in the cortical parenchyma and the pith (Fig. 5, A and G). LM6 epitopes were more abundant in vascular bundles with an active intrafascicular cambium (Fig. 5B) than without (Fig. 5A). Within the vascular bundles, labeling was observed in the cambial region, phloem, and xylem parenchyma cells in close contact with xylem vessels (Fig. 5B). No signal was observed in cells with secondary walls including xylem vessels (Fig. 5I) and interfascicular fibers (data not shown).

In the *araf1-1* mutant, no qualitative differences in the cell types that were labeled with LM6 were observed. However, an increase in labeling intensity was observed in all cell types (Fig. 5, D versus A and E versus B). In vascular bundles, labeling was intense in the walls of parenchyma cells in close contact with vessels (Fig. 5, J versus I). Labeling was also more intense in the cortical parenchyma (Fig. 5, H versus G) and the pith (data not shown). In the apical portion of the wild-type stems, LM6 labeling was uniformly very low, with the exception of the epidermis, suggesting that α-(1,5)-arabinans are present in very low amounts at this stage of stem development. No differences in LM6 signal intensity were observed in the *araf1-1* mutant in this tissue (data not shown).

In wild-type roots, LM6 labeling was detected in the phloem, cambial region, and parenchyma cells in close association with xylem vessels (Fig. 5C). The epidermal and cortical parenchyma cell walls showed barely detectable LM6 labeling. No labeling was detected in xylem vessel walls. Again, in the *araf1-1* mutant root, although no qualitative differences in LM6 labeling were detected, signal intensity was higher in all cell types (Fig. 5, F versus C).

Table I. *Monosaccharide composition of AIR from wild-type, mutant, and overexpressing lines*

The differences among lines that are discussed in the text are indicated in boldface. *araf1-1* is in the Ws background, whereas *35S::ARAF1a*, *35S::ARAF1b*, and *35S::ARAF1c* are in the Col0 background. Comparisons should be made accordingly. Results are means of duplicate determinations and are expressed in moles for 100 mol of monosaccharides in the AIR. SD values are shown in parentheses. For a given monosaccharide, means with the same letter (a–e) are not significantly different based on Fisher's LSD mean comparison test. L-Fuc was detected in all samples, but the amount was lower than 0.4 mol % in stems and 0.6 mol % in roots and seeds.

Monosaccharide	Ws	*araf1-1*	Col0	*35S::ARAF1a*	*35S::ARAF1b*	*35S::ARAF1c*
Seed						
L-Rhamnose	7.0 (0.2) ab	6.7 (0.1) a	6.4 (0.6) a	7.8 (0.4) c	7.7 (0.01) bc	7.7 (0.1) bc
L-Ara	**13.7 (0.2) c**	**15.0 (0.2) d**	**13.9 (0.2) c**	**12.8 (0.3) ab**	**13.3 (0.2) bc**	**12.3 (0.4) a**
D-Xyl	4.6 (0.1) ab	4.7 (0.1) ab	4.9 (0.3) b	4.6 (0.01) ab	4.8 (0.1) ab	4.5 (0.1) a
D-Man	2.6 (0.05) a	2.6 (0.04) a	2.5 (0.03) a	2.6 (0.08) a	3.4 (0.9) a	2.8 (0.2) a
D-Gal	11.5 (0.5) a	11.7 (0.2) a	11.6 (0.5) a	11.6 (0.2) a	11.9 (0.2) a	11.5 (0.4) a
D-Glc	27.5 (1.3) a	25.7 (0.5) a	26.5 (2.2) a	25.4 (0.5) a	25.4 (0.3) a	25.7 (0.2) a
Uronic acids	32.3 (1.3) a	33.1 (0.2) a	33.7 (3.9) a	34.7 (0.4) a	32.9 (0.7) a	35.0 (1.4) a
Root						
L-Rhamnose	1.6 (0.01) b	1.6 (0.01) b	1.5 (0.1) b	1.1 (0.02) a	1.1 (0.01) a	1.5 (0.2) b
L-Ara	4.5 (0.3) ab	4.2 (0.3) a	5.4 (0.03) c	4.9 (0.3) bc	5.3 (0.4) c	6.5 (0.2) d
D-Xyl	14.3 (0.03) b	14.8 (0.4) b	**12.9 (0.1) a**	**16.2 (0.2) c**	**15.1 (0.5) b**	**14.6 (1.0) b**
D-Man	2.6 (0.01) cd	2.8 (0.17) d	2.5 (0.02) bc	2.2 (0.05) a	2.3 (0.11) ab	2.7 (0.1) cd
D-Gal	5.3 (0.2) ab	5.3 (0.1) ab	5.8 (0.01) b	5.4 (0.3) ab	5.5 (0.4) b	6.7 (0.3) c
D-Glc	43.7 (2.3) c	45.6 (0.4) c	42.7 (0.01) bc	42.9 (1.6) bc	40.1 (1.2) ab	38.0 (2.6) a
Uronic acids	27.4 (1.7) bc	25.2 (0.2) a	28.7 (0.2) bcd	26.9 (1.0) ab	30.2 (0.8) d	29.4 (0.7) cd
Stem (upper)						
L-Rhamnose	1.3 (0.01) e	1.3 (0.01) e	1.1 (0.05) d	1.0 (0.01) b, c	0.9 (0.05) b	1.0 (0.03) c
L-Ara	3.6 (0.04) d	3.8 (0.1) d	2.4 (0.1) b	2.4 (0.05) b	2.3 (0.1) b	2.7 (0.04) c
D-Xyl	12.1 (0.2) a	12.3 (0.2) a	16.1 (0.8) b	16.8 (0.4) bc	18.4 (0.7) d	16.3 (0.6) b
D-Man	3.2 (0.1) ab	3.3 (0.04) b	3.1 (0.1) ab	3.1 (0.1) ab	3.2 (0.1) b	3.3 (0.2) b
D-Gal	5.5 (0.1) d	5.9 (0.2) d	3.8 (0.2) c	3.3 (0.03) b	3.3 (0.1) b	3.9 (0.1) c
D-Glc	44.7 (2.1) a	45.1 (0.7) a	54.5 (0.6) bc	56.3 (0.1) c	54.8 (1.7) c	51.9 (0.2) b
Uronic acids	29.2 (2.6) d	27.8 (0.6) d	18.8 (0.6) bc	16.9 (0.2) ab	16.9 (0.8) ab	20.6 (1.1) c
Stem (lower)						
L-Rhamnose	0.8 (0.01) ab	0.8 (0.04) ab	1.0 (0.05) c	0.9 (0.01) c	0.8 (0.02) a	0.8 (0.01) ab
L-Ara	1.4 (0.1) abc	1.2 (0.1) a	1.5 (0.1) c	1.4 (0.1) bc	1.3 (0.01) ab	1.3 (0.02) ab
D-Xyl	19.6 (0.1) cd	19.5 (0.4) c	**17.5 (0.2) a**	**18.6 (0.05) b**	**20.1 (0.3) d**	**19.2 (0.1) c**
D-Man	3.4 (0.02) e	3.4 (0.02) e	2.5 (0.1) a	2.7 (0.01) cd	2.8 (0.01) d	2.7 (0.03) bc
D-Gal	2.2 (0.04) bc	2.0 (0.1) a	2.7 (0.1) e	2.5 (0.05) d	2.2 (0.1) abc	2.4 (0.1) cd
D-Glc	55.2 (0.1) a	57.2 (2.3) ab	56.9 (1.2) ab	58.9 (0.2) b	58.7 (0.9) b	58.9 (1.5) b
Uronic acids	17.2 (0.1) bc	15.7 (2.4) abc	**17.6 (0.7) c**	**14.8 (0.3) abc**	**13.9 (0.6) a**	**14.5 (1.4) ab**

As a complementary means to assess the link between ARAF1 and LM6 epitopes, resin-embedded sections of wild-type stems were incubated with ARAF1 enzyme or a commercial arabinofuranosidase from *Aspergillus niger*. This resulted in a nearly complete loss of LM6 signal (Fig. 6). These results, together with the mutation-induced increase of LM6 labeling, suggest that LM6 epitopes are likely to be in vivo ARAF1 substrates. Unexpectedly, however, we were unable to detect significant variations in LM6 signal localization or intensity compared with the wild type in any tissues in the three independent *35S::ARAF1* lines (data not shown).

As LM6 has been shown to bind pectic arabinan but also some proteins, presumably arabinogalactan proteins (Lee et al., 2005; Harholt et al., 2006), the observed differences in LM6 labeling could be due to a difference in the amount of pectic arabinan, protein arabinan, or both. To determine whether the amount of protein arabinan is altered in mutant or ARAF1-overexpressing lines, ELISAs using the LM6 antibody were performed on total protein extracts from the lower part of stems of wild-type, *araf1* mutant, and *35S::ARAF1* lines. No significant differences in the quantity of LM6 epitopes could be detected (Fig. 7), suggesting that the absence or overexpression of ARAF1 does not alter the structure of the arabinan moiety of proteins. These data, together with immunolocalization, argue in favor of the arabinan component of pectins rather than proteins as the potential in vivo substrate of ARAF1.

Because in vitro assays suggested that ARAF1 can hydrolyze L-Ara and D-Xyl present in arabinoxylans (Minic et al., 2006), we tested the effect of modified ARAF1 expression on the distribution and amounts of xylan using LM10 and LM11 antibodies (McCartney et al., 2005). The general belief is that LM10 recognizes low-substituted arabinoxylans whereas LM11 recognizes both low- and higher-substituted arabinoxylans (Carafa et al., 2005; Bauer et al., 2006; Zhou et al., 2006). In Arabidopsis stems, LM10 and LM11 signals are found in cells with secondary walls (http://www.bmb.leeds.ac.uk/staff/jpk/gal5.htm; Bauer et al., 2006; Zhou et al., 2006). In agreement with these results, we detected

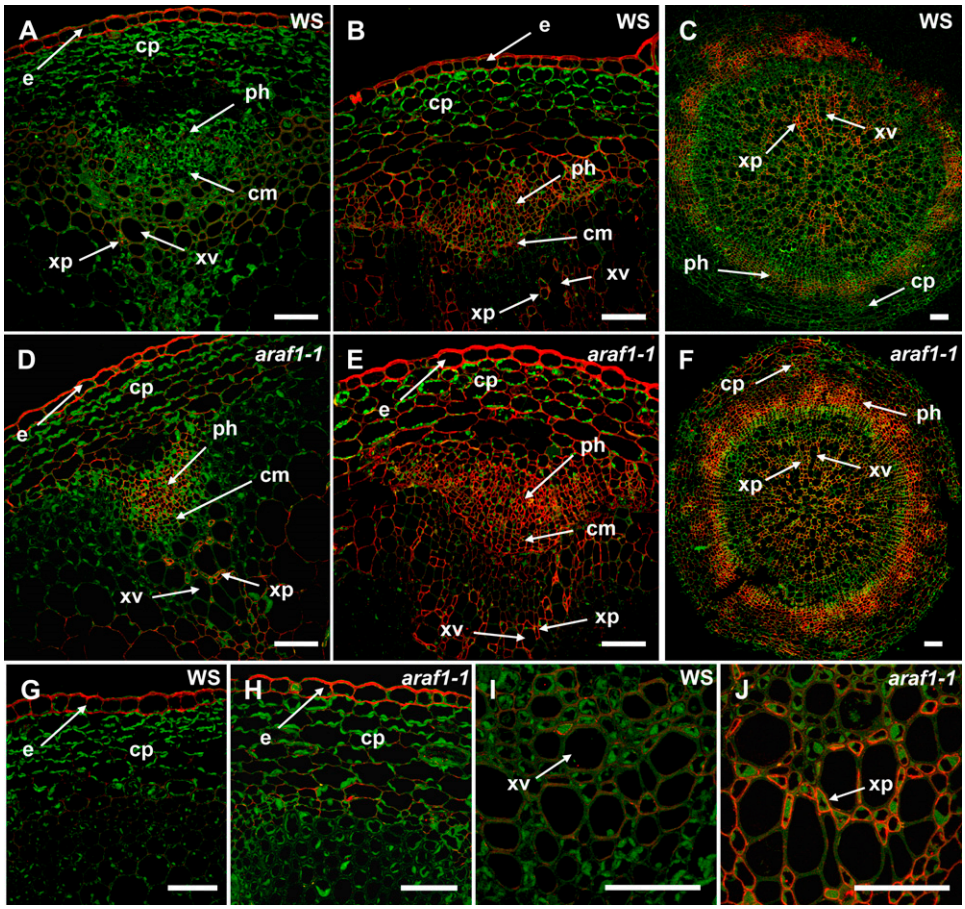

Figure 5. Indirect immunofluorescence micrographs of resin-embedded Ws (A, B, C, G, and I) and *araf1-1* (D, E, F, H, and J) stem (A, B, D, and E) and root (C and F) sections labeled with LM6 monoclonal antibody. LM6 signal and autofluorescence of tissues at 488 nm are indicated by the red and green color scales, respectively. LM6 signal intensity is higher in *araf1-1* stems (compare D versus A and E versus B) and roots (compare F versus C) independent of the presence of an active cambium (compare B versus A). Signal was also higher in the cortical parenchyma (compare H versus G) and in the xylem parenchyma in contact with vessels (compare J versus I). cm, Cambium; cp, cortical parenchyma; e, epidermis; ph, phloem; xp, xylem parenchyma; xv, xylem vessel. Bars represent 50 μm.

LM10 label in xylary and interfascicular fibers and in xylem vessels in the basal portion of wild-type stems (Fig. 8A). One to two layers of parenchyma cells in the pith and in the cortex adjacent to interfascicular fibers were also labeled (Fig. 8A, dashed arrows). In ARAF1-overexpressing lines, although the distribution of the LM10 signal was not modified, the intensity was enhanced significantly (Fig. 8, B versus A). The difference in signal intensity was greater in *35S::ARAF1b* and *35S::ARAF1c* than in the *35S::ARAF1a* line (data not shown). This correlated with the more enhanced arabinofuranosidase activity measured in these lines (Fig. 3B). No differences in LM10 labeling were observed in the *araf1-1* mutant (data not shown). This is perhaps not surprising because *ARAF1* is not normally expressed in LM10-containing cell types.

In wild-type roots, LM10 epitopes were localized exclusively in cells within the stele (Fig. 8C). In the outermost portion of the xylem, vessels and fibers were labeled, whereas in the inner part of the xylem, the signal was restricted to the vessels. In ARAF1-overexpressing roots, as is the case in stems, LM10 signal intensity was increased significantly, although no change in distribution was observed (Fig. 8D). Again, LM10 labeling was unchanged in the *araf1-1* mutant (data not shown). Using the LM11 antibody, similar increases in signal intensity were observed for all lines and tissues examined (data not shown).

The increase of LM10 and LM11 labeling in *35S::ARAF1* transformants suggested that ARAF1 is able to alter xylan composition. To determine the effect of arabinofuranosidase activity on LM10 and LM11 binding, resin-embedded sections of the lower part of the stem from wild-type plants were treated with ARAF1 or a commercial *A. niger* arabinofuranosidase and subsequently labeled with LM10 or LM11 antibodies. The commercial arabinofuranosidase from *A. niger* is reported to hydrolyze L-Ara, but not D-Xyl, from wheat arabinoxylan. Arabinofuranosidase treatment of sections did not alter LM10 or LM11 signal intensity (data not shown), suggesting that, at least at this particular stage of stem development, neither of the arabinofuranosidases altered the LM10 or LM11 epitope structures. Alternatively, the increase in LM10 and LM11 signal in the ARAF1 overexpressors may be due to an increase in xylan content, as indicated by monosaccharide analysis or structural secondary wall modifications leading to increased antibody accessibility to xylan.

Transcriptomic Analysis of *araf1-1* and *35S::ARAF1b*

Pairwise transcriptomic comparisons of the basal portion of stems were performed on Ws versus *araf1-1* and Col0 versus *35S::ARAF1b* using the complete Arabidopsis transcriptome microarray (CATMA; Crowe

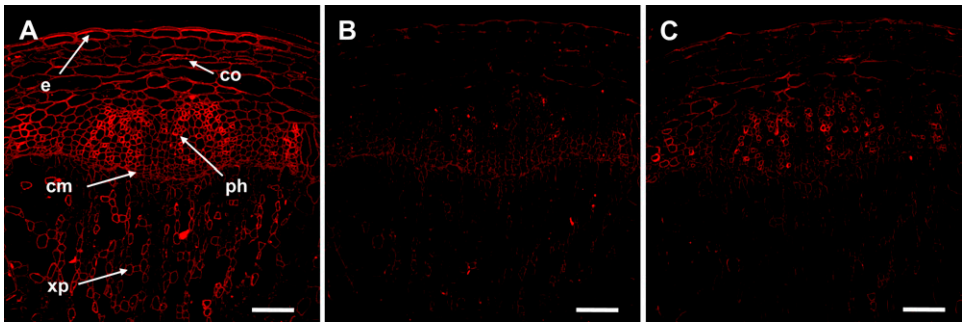

Figure 6. In-section arabinofuranosidase activity assays and subsequent LM6 labeling. LR White resin-embedded sections were treated with buffer (A), partially purified ARAF1 (B), or a commercial arabinofuranosidase from *A. niger* (C) and subsequently labeled with the LM6 antibody. The LM6 signal is represented by the red color scale. Autofluorescence of tissues at 488 nm was omitted. e, Epidermis; cm, cambium; co, cortex; ph, phloem; xp, xylem parenchyma. Bars represent 50 μm. [See online article for color version of this figure.]

et al., 2003). The CATMA contains 24,576 sequences corresponding to known and predicted genes. The *araf1-1* mutation had only a very minor impact on global gene expression, in keeping with the subtle cell-specific wall modifications (Supplemental Table S1). Among the 54 differentially expressed genes, six that are classified in the CAZY database were up-regulated 2- to 3-fold: a putative β-amylase (At5g18670), an endo-xyloglucan transferase (AtXth4; At2g06850), a putative β-galactosidase (At5g56870), a putative α-galactosidase (At5g20250), and two putative trehalose-P synthases, *TPS2* (At1g70290) and *TPS11* (At2g18700). Four genes participating in hormone metabolism or hormone response were also found to be differentially expressed in *araf1-1*. None of the genes associated with global L-Ara metabolism, including L-arabinosyl-transferases and Ara-kinases, exhibited differential expression as a result of the *araf1* mutation.

In contrast to *araf1-1*, the overexpression of ARAF1 resulted in far-reaching effects on global gene expression, with 1,784 differentially expressed genes in *35S::ARAF1b* (Supplemental Table S2). Fifty of them are classified in the CAZY database. Among them are genes with a putative role in L-Ara metabolism, including the other arabinofuranosidase family 51 member, *ARAF2* (At5g26120), which was up-regulated, and a putative endo-arabinanase (At5g67540), which was down-regulated (Table II). No GH family 3 members or putative β-1,4-xylanases were differentially expressed. The putative functions of the CAZY genes that were differentially regulated in *35S::ARAF1b* were highly variable; they included putative pectin methyl-esterases, putative family 1 pectate-lyases, several β-glucosidases, and several glucosyl-transferases. We also found three down-regulated trehalose-P synthases, *TPS1* (At1g78580), *TPS7* (At1g06410), and *TPS11* (At2g18700; Table II). *TPS1* has been shown to participate in the regulation of carbon metabolism and the transition from the vegetative to the reproductive stage in Arabidopsis (Schluepmann et al., 2003; van Dijken et al., 2004). Many genes involved in secondary wall metabolism were also differentially expressed (Table II). They included genes encoding enzymes of the shikimate (a putative chorismate synthase, a putative dehydroquinate dehydratase, and a hydroxy-cinnamoyltransferase) and phenylpropanoid (among them were two Phe ammonia-lyases, including *PAL1*, cinnamoyl-CoA reductase 1 and 2, a putative 4-coumaroyl-CoA synthase, and a cinnamic acid 4-hydroxylase) pathways. Furthermore, Bglu45 (At1g61810), a monolignol β-glucosidase, was also down-regulated. These results suggest that the alteration of polysaccharide metabolism leads to the regulation of the lignin biosynthetic pathway. However, UV autofluorescence and phloroglucinol staining of the lower part of the stem fresh sections did not reveal any alterations in lignin distribution in any of the *35S::ARAF1* lines (data not shown). Finally, a large number of genes participating in hormone metabolism, in particular auxin, abscisic acid, and ethylene, and genes involved in abiotic stimuli response and plant-microorganism interactions, were also among the differentially expressed genes in *35S::ARAF1b*. These are presumably indirect consequences of increased ARAF1 activity on global gene expression and suggest that the modification of cell wall structure may have important consequences in plant development and responses to the environment.

DISCUSSION

Pectic Arabinans Are Potential in Vivo ARAF1 Substrates in Arabidopsis

In this study, we have determined the sites of *ARAF1* gene expression at the cellular level and, in combination with genetic and immunochemical approaches, have identified pectic arabinans as potential in vivo substrates of ARAF1. *ARAF1* is expressed in vascular tissues, including the cambium, phloem, and xylem parenchyma cells, and is largely overlapping with LM6 labeling in wild-type plants. In-section assays in which wild-type stem sections were treated with ARAF1 enzyme resulted in the nearly complete disappearance of LM6 signal. In addition, in ARAF1-deficient plants,

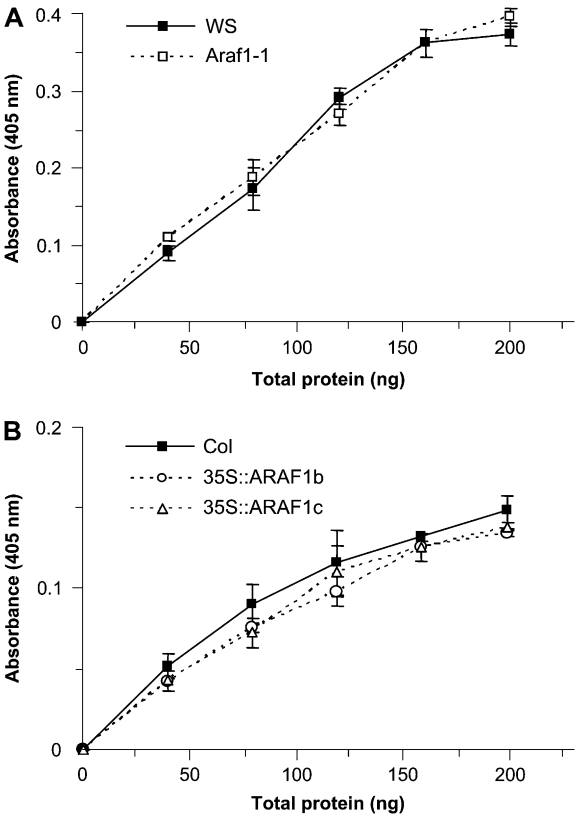

Figure 7. ELISA quantification of LM6-reactive proteins in crude stem extracts. A, Ws (black squares) and *araf1-1* (white squares). B, Col0 (black squares), *35S::ARAF1b* (white circles), and *35S::ARAF1c* (white triangles). It should be noted that the same results were obtained for *35S::ARAF1a*. For clarity, only *35S::ARAF1b* (white circles) and *35S::ARAF1c*, the two lines with the highest ARAF activity, are shown in B. Each series of measurements was performed with three plants per line. Error bars indicate SD.

an increase in LM6 labeling was observed, suggesting that the absence of ARAF1 causes the accumulation of LM6 epitopes. As indicated by ELISA using crude protein extracts, this increase was not due to an increase in LM6 epitope-containing glycoproteins. Furthermore, Harholt et al. (2006) have shown that an important proportion of the LM6 signal in the stem can be attributed to the arabinan component of rhamnogalacturonan-I. Finally, biochemical data indicate that pectic arabinan is a substrate of ARAF1 in vitro (Minic et al., 2004, 2006). Together, these results suggest that pectic arabinans are potential substrates of ARAF1 in vivo.

Unexpectedly, *35S::ARAF1* lines showed no reduction in LM6 signal intensity. One explanation could be that, in muro, ARAF1 alone cannot fully hydrolyze arabinans and that the wild-type ARAF1 enzyme is already hydrolyzing LM6 epitope-containing wall components at a maximal rate. This scenario is not likely because wild-type stem sections treated with native Arabidopsis ARAF1 resulted in the complete disappearance of LM6 signal, suggesting that ARAF1 can indeed completely hydrolyze arabinans when present in sufficient quantities. Another more plausible explanation is that fine-tuning mechanisms are controlling arabinan dynamics at the cell wall. The existence of such mechanisms is apparent when considering a wild-type plant. LM6 signal is readily detected in cells, despite the presence of ARAF1, which hydrolyzes arabinans in these same cell types. An equilibrium between active arabinofuranosidases and arabinan-containing substrates has already been described in Arabidopsis microcalli cultures (Leboeuf et al., 2004). It is possible that an increase in ARAF1 activity in the overexpressing lines might accelerate the rate of overall arabinan cycling; that is, not just hydrolysis but also reincorporation into wall polysaccharides, without having an impact on their final content and/or structure. L-[^{3}H]Ara or [^{14}C]Ara feeding experiments in proso millet (*Panicum miliaceum*), maize (*Zea mays*; Gibeaut and Carpita, 1991), and Arabidopsis (Dolezal and Cobbett, 1991; Burget et al., 2003) showed that L-Ara is actively cycled between a monosaccharide and a polysaccharide state, suggesting that arabinans are undergoing constant remodeling. A final argument for fine-tuning mechanisms in cell wall arabinan metabolism is that biosynthetic and hydrolytic enzymes are at least partially colocalized in the same cell types. For example, *ARAD1*, a putative pectin arabinosyltransferase, is expressed in certain *ARAF1*-expressing cell types in stems and roots (Harholt et al., 2006). Interestingly, the overexpression of *ARAD1* in a wild-type background did not lead to an increase in L-Ara content in the cell wall, suggesting that arabinan biosynthesis is not regulated at the transcriptional level of glycosyltransferase genes. A detailed analysis of the possible interactions between arabinan hydrolytic and biosynthetic pathways would help in understanding what determines cell wall L-Ara content.

Localized Arabinan Alterations Do Not Lead to a Visible Phenotype

When considering the restricted cell-specific *ARAF1* gene expression, it is perhaps not surprising that ARAF1-deficient plants did not exhibit major differences in cell wall global monosaccharide composition, particularly L-Ara, under normal growth conditions. The cell-specific localization of *ARAF1* may also explain the limited number of genes that were differentially expressed in the *araf1-1* mutant background. Two mutants with reduced L-Ara content, *mur4* and *arad1*, have been characterized previously. *arad1* is affected in an arabinosyltransferase gene and is characterized by a 70% reduction in the L-Ara content of the rhamnogalacturonan-I fraction (Harholt et al., 2006). *mur4* is a mutant of a UDP-D-Xyl4-epimerase and has a 50% to 75% reduction in L-Ara content that affects not only pectic arabinan but also other L-Ara-containing molecules such as rhamnogalacturonan-II and arabinogalactan proteins (Burget and Reiter, 1999; Burget et al., 2003). Similar to *araf1*, neither of these mutants exhibits

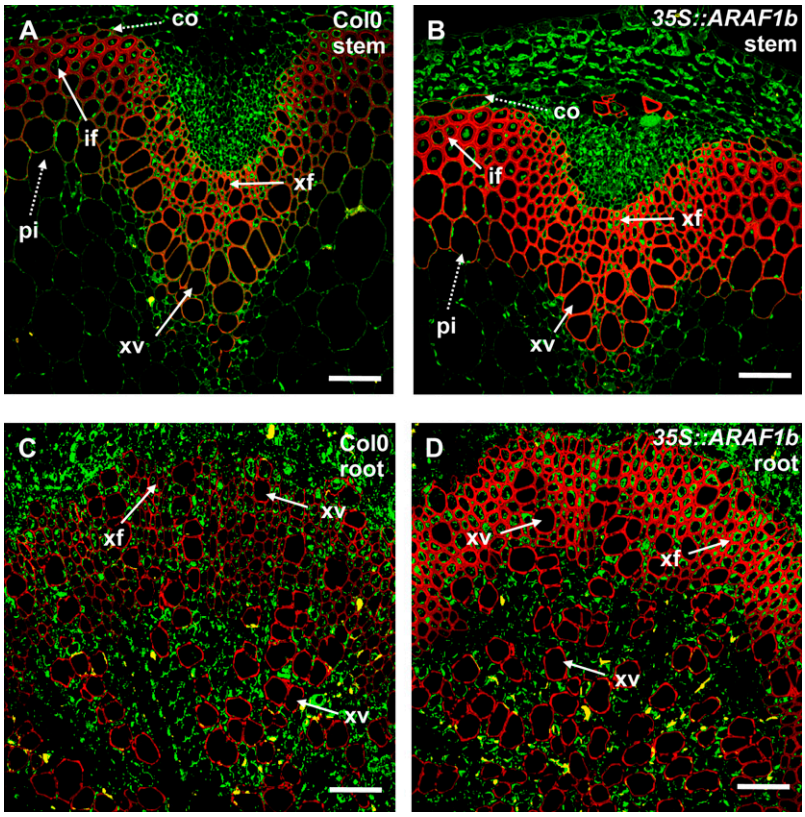

Figure 8. Indirect immunofluorescence micrographs of resin-embedded Col0 and *35S::ARAF1b* stem (A and B) and root (C and D) sections labeled with the LM10 monoclonal antibody. LM10 signal and autofluorescence of tissues at 488 nm are indicated by the red and green color scales, respectively. In the lower part of the stem, LM10 signal is found in metaxylem vessels, secondary xylem, and interfascicular fibers. Dashed arrows indicate cortical and pith cells that also show LM10 labeling. In roots, LM10 signal is found exclusively in xylem fibers and xylem vessels. co, Cortex; if, interfascicular fiber; pi, pith; xf, xylem fiber; xv, xylem vessel. Bars represent 50 μm.

an apparent phenotype. Together, these results indicate that a large plasticity is tolerated in the amount of L-Ara present not only in arabinans but also in a wider range of L-Ara-containing molecules. Other structural features of pectins besides arabinan composition appear to be more critical for normal plant development. For example, the *qua1* mutant, which is defective in a family 8 putative glycosyltransferase, exhibited a reduction of 25% in homogalacturonan, resulting in a wide range of phenotypic defects, including dwarfing and a loss of cell adhesion (Bouton et al., 2002; Leboeuf et al., 2004). The *mur1 mur4* double mutant has an extreme dwarfed phenotype that has been attributed to defects in rhamnogalacturonan-II structure (Burget et al., 2003).

Although arabinan has been shown to play an important role in guard cell function in isolated epidermal strips treated with exogenous fungal endo-arabinanse (Jones et al., 2003), it is unclear whether endogenous arabinan-remodeling enzymes actually participate in this process. Guard cell function was not affected in either *araf1* (S. McQueen-Mason, personal communication) or *arad1* mutants, although in the latter case it is unknown whether *ARAD1* is expressed in guard cells (Harholt et al., 2006). It would be of interest to determine whether the overexpression of an endogenous arabinanase with a major impact on LM6 labeling would affect stomatal function.

Another important factor that may explain a lack of visible phenotype in *araf1* mutants is the presence of other arabinofuranosidase activities with overlapping spatiotemporal expression that may compensate for ARAF1 activity. In Arabidopsis stems, there are at least two other enzymes that fit these criteria: XYL1 (encoded by At5g49360) and ARAF2 (encoded by At5g26120). Although XYL1 is a GH family 3 member, its biochemical characteristics are almost identical to those of ARAF1 (Minic et al., 2004). Genevestigator database mining indicated nearly identical organ expression between the two genes (https://www.genevestigator.ethz.ch/). Furthermore, the analysis of *pXYL1::GUS* plants showed that *XYL1* is expressed in the fibers, protoxylem, metaxylem, and intrafascicular cambium but not in the phloem (Goujon et al., 2003). ARAF2 is a family 51 GH with 78% identity to ARAF1 and has been shown to hydrolyze pNPA (Z. Minic and L. Jouanin, unpublished data). Analysis of *pARAF2::GUS* plants indicated that *ARAF2* is expressed in the cambium and phloem but not in the xylem (R.A. Chávez Montes and D. Goffner, unpublished data). The partially overlapping expression patterns of these enzymes suggest that functional redundancy is plausible in some cell types. That said, the *araf2* single mutant exhibited no apparent phenotype, and more importantly, the phenotype of *araf1 araf2* double mutants was not additive compared with that of the single *araf1-1* mutant (data not shown), suggesting that compensation by ARAF2 in the *araf1* mutant background was unlikely. Compensation by other family 3 or even family 43 GHs, however, cannot be excluded because there is no information currently available on the expression or substrate specificity of these enzymes.

Table II. *List of selected CAZY and lignin-related genes differentially expressed in 35S::ARAF1b stems*

Genes are identified by their Arabidopsis Genome Initiative (AGI) number. The ratio indicates signal hybridization intensities of *35S::ARAF1b* versus Col0 expression.

Gene Description	AGI No.	CAZY Family	Ratio	*P*
CAZY genes				
Pectin methyl esterase	At1g11580	CE08	0.42	0.0000
Pectin methyl esterase	At2g26440	CE08	0.58	0.0218
Pectin methyl esterase	At3g43270	CE08	0.57	0.0074
Pectin methyl esterase	At5g09760	CE08	1.71	0.0310
β-Glucosidase	At1g26560	GH01	0.19	0.0000
β-Glucosidase	At1g52400	GH01	0.43	0.0000
Monolignol β-glucosidase	At1g61810	GH01	0.52	0.0001
β-Glucosidase	At2g44450	GH01	0.56	0.0037
β-Glucosidase	At2g44490	GH01	0.53	0.0002
β-Mannosidase	At3g18080	GH01	2.51	0.0000
β-Glucosidase	At3g60120	GH01	0.44	0.0000
β-Glucosidase	At3g60130	GH01	0.53	0.0003
Endo-arabinanase	At5g67540	GH43	0.57	0.0094
α-L-Arabinofuranosidase	At5g26120	GH51	2.86	0.0000
Glucosyl-transferase	At1g06000	GT01	0.55	0.0010
Glucosyl-transferase	At2g18560	GT01	1.99	0.0000
Glucosyl-transferase	At3g11340	GT01	0.58	0.0238
Glucosyl-transferase	At5g12890	GT01	0.34	0.0000
Glucosyl-/galactosyl-transferase	At3g02350	GT08	0.41	0.0000
Glucosyl-/galactosyl-transferase	At3g58790	GT08	0.57	0.0098
Glucosyl-/galactosyl-transferase	At5g18480	GT08	0.44	0.0000
Trehalose-P synthase	At1g06410	GT20	0.56	0.0035
Trehalose-P synthase	At1g78580	GT20	0.45	0.0000
Trehalose-P synthase	At2g18700	GT20	0.39	0.0000
Glucosyl-transferase	At3g02230	GT75	0.39	0.0000
Glucosyl-transferase	At5g15650	GT75	0.32	0.0000
Pectate lyase	At3g01270	PL1	1.70	0.0378
Pectate lyase	At3g27400	PL1	0.42	0.0000
Pectate lyase	At4g24780	PL1	1.80	0.0027
Lignin genes				
Shikimate metabolism				
Chorismate synthase	At1g48850		0.54	0.0004
3-Dehydroquinate dehydratase	At3g06350		0.57	0.0118
Phe metabolism				
Phe ammonia-lyase	At2g37040		0.30	0.0000
Phe ammonia-lyase	At3g10340		0.46	0.0000
Prephenate dehydratase	At5g22630		0.56	0.0030
Phenylpropanoid metabolism				
Cinnamoyl-CoA reductase	At1g15950		0.51	0.0000
Cinnamoyl-CoA reductase	At1g80820		0.33	0.0000
Cinnamic acid 4-hydroxylase	At2g30490		0.27	0.0000
Coumarate 3-hydroxylase	At2g40890		0.37	0.0000
S-adenosyl-Met synthetase	At3g17390		0.33	0.0000
Oxidoreductase. 2OG-Fe(II) oxygenase family protein	At3g19010		0.44	0.0000
4-Coumarate-CoA ligase	At3g21230		0.32	0.0000
Oxidoreductase. 2OG-Fe(II) oxygenase family protein	At5g24530		0.42	0.0000
Hydroxycinnamoyl-CoA shikimate/quinate hydroxycinnamoyltransferase	At5g48930		0.43	0.0000
Monolignol metabolism				
Monolignol β-glucosidase	At1g61810		0.52	0.0001

However, transcriptomic comparisons between *araf1-1* and wild-type plants suggest that compensation mechanisms are not regulated at the transcriptional level because none of the above-mentioned GHs exhibited increased expression in mutant lines. In any case, it would be of interest to characterize other combinatorial mutants to assess the effects of different arabinan modifications on plant development and to determine to what extent these enzymes may work in a coordinated manner in remodeling pectin structure.

Ectopic Expression of ARAF1 Leads to Secondary Wall Alterations and a Developmental Phenotype

The increase in LM10 and LM11 labeling intensity in the secondary walls of *35S::ARAF1* lines is intriguing. Although there are several possible explanations, none of them provides information regarding the in vivo substrate of ARAF1, because these wall modifications occurred in cell types in which *ARAF1* is not normally expressed. One possibility is that the ectopic overexpression of *ARAF1* could lead to the excess hydrolysis of arabinosyl residues of arabinoxylans in secondary walls. This would result in a decrease in the degree of substitution of arabinoxylans and would thereby generate more low and nonsubstituted xylans (epitopes of LM10 and LM11) and/or enhance antibody accessibility to the epitopes. In keeping with this hypothesis, it has been shown that ARAF1 hydrolyzes L-Ara from arabinoxylans in vitro (Minic et al., 2004, 2006). However, if this were true, one would expect an increase in LM10 and LM11 labeling in ARAF1-treated sections, and this was not the case. Moreover, recent mass spectrometry analysis has shown that xylans present in mature Arabidopsis stems are glucuronoxylans rather than arabinoxylans (L. Jouanin, unpublished data). Interestingly, the overexpressing lines exhibit an increase in D-Xyl content in roots and stems, and perhaps this in itself is sufficient to explain an increase in LM10 and LM11 signal in these organs. In this case, altered secondary wall structure is most likely an indirect consequence of ARAF1 overexpression.

Comparative transcriptomic analysis of *35S::ARAF1* lines indicates that ARAF1 overexpression has far-reaching consequences on global gene expression, some of which could be associated with changes in secondary cell wall structure. For example, several key genes involved in monolignol biosynthesis are down-regulated in *35S::ARAF1b* stems. This could result in an altered lignin network that, in turn, could lead to enhanced accessibility of LM10 and LM11 epitopes. However, UV autofluorescence and phloroglucinol staining of *35S::ARAF1a*, *-b*, and *-c* stems did not reveal any major alterations in lignin distribution in these lines. A detailed analysis of the modified pathways in the *35S::ARAF1* lines will be necessary to determine the causal relationship between ARAF1 overexpression and secondary cell wall alterations.

A developmental phenotype was observed when ARAF1 was ectopically expressed in Arabidopsis. In *35S::ARAF1* lines, a delay in inflorescence emergence and fewer secondary stems were observed. Similarly, potato (*Solanum tuberosum*) plants overexpressing an *A. niger* endo-arabinanase exhibited altered stem architecture, flowering defects, and even starch accumulation in the stem (Skjøt et al., 2002; Borkhardt et al., 2005). Together, these results suggest a close relationship between arabinans, carbon status, and overall plant development. Stem emergence is the result of a vegetative-to-reproductive stage transition and is controlled by hormone (Koornneef et al., 1998) and metabolic (mostly carbon status) levels. In particular, trehalose has been shown to be important for this transition (van Dijken et al., 2004). Interestingly, in the *35S::ARAF1b* line, three trehalose-P synthases, *TPS1* (At1g78580), *TPS7* (At1g06410), and *TPS11* (At2g18700), were all down-regulated. Moreover, many hormone-related genes were also differentially expressed. The observed delay in inflorescence emergence in the *35S::ARAF1* lines may be the result of these transcriptional modifications.

The Role of ARAF1 Is Likely To Be Cell Type-Dependent

Although expression of the zinnia and hybrid aspen (*Populus tremula* × *Populus tremuloides*) *ARAF1* homologs has been shown to be correlated with xylem differentiation (Demura et al., 2002; Aspeborg et al., 2005; Pesquet et al., 2005), the expression of *ARAF1* in cell types with distinct cellular functions suggests a cell type-specific role for ARAF1. Besides vascular tissues such as phloem, intrafascicular cambium, and xylem, *ARAF1* is also expressed in guard cells, root tips, trichomes, newly emerging leaves, floral abscission zones (Fulton and Cobbett, 2003), and developing embryos (Gomez et al., 2006). Interestingly, coexpression analysis of *ARAF1* and *ARAF2* in plant organs, tissues, and mutants using the Expression Angler from the University of Toronto (http://bbc.botany.utoronto.ca/ntools/cgi-bin/ntools_expression_angler.cgi) on NASCArrays indicated that among genes that had the highest degree of coexpression with *ARAF1* were four cell wall-related genes: *UGE1* (At1g12780), a UDP-D-Glu/UDP-D-Gal4 epimerase, a Xyl epimerase (At5g57655), *XYL1* (At5g49360), and *FRA8* (At2g28110), whereas for *ARAF2*, no easily identifiable cell wall-related genes exhibited high levels of coexpression. The integration of gene expression data at the cellular level, enzymatic characterization, and detailed cell wall composition analyses of plants with modified family 3 and 51 arabinofuranosidase activities should enable us to identify their in vivo substrates and understand their roles in plant physiology.

MATERIALS AND METHODS

Plant Materials and Growth Conditions

Arabidopsis (*Arabidopsis thaliana*) ecotypes Ws and Col0 were used in this work. Two insertional mutants for the At3g10740 gene, *araf1-1* and *araf1-2*, were obtained. *araf1-1*, a mutant in the Ws background, was obtained from the T-DNA insertion line FLAG_091G07 of the Versailles collection. *araf1-2*, a mutant in the Col0 background, was obtained from the T-DNA insertion line GABI_204A04 of the GABI-Kat collection. T3 homozygous mutant lines were identified by PCR. For *araf1-1*, gene-specific primers hmz-araf1-1-F (5′-TCAGGTGGAACCCTGATGCA-3′) and hmz-araf1-1-R (5′-GGAATGTGGCGGGAGAACAA-3′) and the insert-specific primer LBver (5′-CGGCTATTGGTAATAGGACACTGG-3′) were used. The wild-type form of the gene was detected with the hmz-araf1-1 primers, and T-DNA insertion was detected with the hmz-araf1-1-R and LBver primers. For *araf1-2*, gene-specific primers hmz-araf1-2-F (5′-CCAGTATCATGCCCTTTGTT-3′) and hmz-araf1-2-R (5′-CAAAGCCTGGGAAGAGAAAT-3′) and the insert-specific primer LB-o8409 (5′-ATATTGACCATCATACTCATTGC-3′) were used. The wild-type form of the gene was detected with the hmz-araf1-2 primers, and T-DNA insertion was detected with the hmz-araf1-2-R and LB-o8409 primers.

Wild-type and mutant plants were grown in soil in growth chambers at 22°C (day) and 20°C (night) with 16 h of light and 70% humidity. Adult plants were 6 to 7 weeks old with a 40- to 45-cm-high main stem. Stem emergence (i.e. appearance of the first flower buds) is defined as growth stage 5.10 as described by Boyes et al. (2001). Tissue was frozen in liquid nitrogen, ground to a fine powder, and stored at −80°C until use. For some experiments (AIR composition, immunohistochemistry, and ELISA), the main stem was harvested and divided into lower and upper parts. The lower and upper parts of the stem corresponded to the bottom and top 10 cm of the main stem, respectively. Stem tissue was devoid of any cauline leaves, siliques, or flowers.

RT-PCR

One milliliter of Extract-All (Eurobio) was added to approximately 100 mg of ground frozen tissue. RNA was isolated according to the Extract-All protocol, then incubated with 5 units of RQ1 RNase-free DNase I (Promega) for 1 h at 37°C and again treated with Extract-All to remove DNase. RNA was quantified spectrophotometrically at 260 nm using a Biophotometer (Eppendorf) and verified by gel electrophoresis. cDNA was generated with 2 μg of RNA using ImPromII reverse transcriptase (Promega). PCR was carried out using the GoTaq Flexi (Promega) protocol with 0.25 μg of cDNA.

For the *araf1-1* mutant, the absence of *ARAF1* transcript was determined using primers rt-araf1-1-F (5′-TGGAACCCTGATGCAATAGT-3′) and rt-araf1-1-R (5′-TCATATCCTCCTCTGCCAAC-3′), resulting in amplicons of 382 bp for cDNA and 539 bp for genomic DNA. Primers hmz-araf1-1 were not used because hmz-araf1-1-F contains part of an intron sequence. Hybrid *ARAF1-T-DNA* transcript was detected using primers hyb-araf1-1 (5′-TCCAAAACCAGCCGTGACTT-3′) and RBver (5′-CTGATACCAGACGTTGCCCGCATAA-3′) with an annealing temperature of 60°C, resulting in amplicons of approximately 2.3 kb for cDNA and 3.8 kb for genomic DNA. For *araf1-2*, transcript absence was determined using primers hmz-araf1-2-F and rt-araf1-2-R (5′-GCCATTGTTTTTCCAAGAGATA-3′) with an annealing temperature of 60°C, resulting in amplicons of 689 bp for cDNA and 1,184 bp for genomic DNA.

pARAF1::*GUS* Plant Analysis

pARAF1::*GUS* plants have been described previously (Fulton and Cobbett, 2003). GUS staining was performed at 37°C in GUS staining solution (50 mM sodium phosphate buffer, pH 7.0, 0.1% Triton X-100, 1 mM potassium ferricyanide, 1 mM potassium ferrocyanide, and 1 mM X-glucuronoside) with 10 min of vacuum infiltration. After staining, the plant tissue was cleared for at least 1 h with ethanol:acetic acid (1:1, v/v) at room temperature, and tissues were kept at 4°C in 70% ethanol until observation.

Transformation of Plants with a *35S*::*ARAF1* Overexpression Construct

The *ARAF1* region from start to stop codon was amplified by RT-PCR from total RNA using gene-specific primers araf1-[+1] (5′-ATGGATATGGAGTCTTGGAAGTTGCTCAGAAG-3′) and araf1-[−1] (5′-TCACACAGTGGTAGTTTTCTGATGGGAAGAAG-3′). The resulting 2,037-bp fragment was cloned into the pGEM-T Easy vector (Promega), resulting in the pGEMT-araf1 vector. This vector was digested with *Eco*RI, and the resulting 2,057-bp fragment was cloned into the *Eco*RI cloning site of a vector derived from vector pGreen0029 (pGreen), pGreen0029-35SCAMΩ (a kind gift from Julie Cullimore, Institut National de la Recherche Agronomique, Toulouse, France), which contains two tandem 35S cauliflower mosaic virus promoters, the nptII kanamycin resistance gene, and a cauliflower mosaic virus terminator. Insert sequence and orientation were verified by sequencing. Col0 plants were transformed by *Agrobacterium tumefaciens* C58-mediated transformation (Clough and Bent, 1998). T1 transformant seeds were grown on selective medium containing kanamycin (100 mg mL^{-1}), and resistant seedlings were transferred to soil and left to self-pollinate. T2 seeds from each plant were harvested and grown on selective medium containing kanamycin, and resistant seedlings from plates with a segregation ratio of 3:1, indicative of a single T-DNA insertion, were transferred to soil and left to self-pollinate. T3 seeds from each plant were harvested, and a sample was grown on selective medium containing kanamycin. Three seed lots with 100% resistance, indicating homozygous transformants, were selected based on the level of *ARAF1* RNA overexpression as assessed by semiquantitative RT-PCR using primers rt-araf1-1. These lines were named *35S*::*ARAF1a* through *35S*::*ARAF1c* and used for subsequent analysis.

α-L-Arabinofuranosidase Activity Assay

Total arabinofuranosidase activity in overexpressing lines was determined in microtiter plates as follows. A crude extract from stem tissue was prepared as described by Minic et al. (2004), and total protein was determined using the bicinchoninic acid method (Sigma). The reaction mixture contained 2 mM pNPA (Fluka), 0.1 M acetate buffer (pH 5.0), and 3.2 μg of protein in a total volume of 0.2 mL. The reaction was carried out at room temperature and stopped at 20-min intervals by the addition of 50 μL of 0.4 M sodium bicarbonate to the assay mixture. The concentration of the product 4-nitrophenol was determined spectrophotometrically at 405 nm, and its amount was estimated from a calibration curve. Specific activity was expressed as the amount of protein required to release 1 nmol min^{-1} 4-nitrophenol.

Cell Wall Preparation and Composition Analysis

AIRs from the upper and lower parts of the stem and roots were prepared as described by Harholt et al. (2006) with slight modifications. Briefly, ground tissue was boiled in 96% ethanol for 30 min. The supernatant was removed after centrifugation for 5 min at 10,000*g*. The pellet was washed eight times with 70% ethanol with subsequent centrifugation. The pellet was then washed twice with 96% ethanol, twice with 100% acetone, and dried in an oven at 40°C overnight. Dry seed AIR was prepared as follows. One hundred to 200 mg of dry seeds from plants grown under the same environmental conditions were frozen in liquid nitrogen and ground to a fine powder. The tissue was boiled in a mixture of chloroform:methanol (1:1, v/v) for 30 min. The supernatant was removed after centrifugation at 10,000*g* for 5 min. The pellet was washed twice with acetone, twice with ethyl ether, and left to evaporate overnight.

The monosaccharide composition of AIRs was determined as their alditol acetates after acid hydrolysis. Samples were prehydrolyzed with 13 M H_2SO_4 for 30 min at 25°C, then H_2SO_4 concentration was adjusted to 1 M with water and samples were hydrolyzed for 2 h at 100°C as described previously (Saulnier et al., 1995). Uronic acids were assayed on the supernatant of acid hydrolysis by the automated *m*-hydroxydiphenyl method (Thibault, 1979) using GalUA as a standard. Analyses were performed in duplicate. One-way ANOVA and mean comparison tests using Fisher's LSD (95% LSD) were used to compare the sugar composition (molar ratio) of the AIR between the wild type, mutants, and transformants.

Immunohistochemistry

Samples of Arabidopsis tissues were fixed in 2.5% (v/v) glutaraldehyde in 50 mM cacodylate buffer (pH 7.0). They were dehydrated in a successive ethanol series (20%, 40%, 60%, 80%, 95%, and 100%) and embedded in LR White resin (Electron Microscopy Sciences; 33%, 50%, 66%, and 100% in ethanol). Thin sections (1 μm) were placed on Teflon-coated slides (Electron Microscopy Sciences), blocked in phosphate-buffered saline, 2% Tween, and 1% bovine serum albumin for 2 h (PBST-BSA), and labeled overnight (12 h) at 4°C with primary antibody diluted in PBST-BSA. Sections were washed with PBST and incubated at room temperature for 2 h with a secondary antibody diluted in PBST-BSA. Slides were then washed with deionized water and dried under a stream of dry air. Primary antibodies and dilutions were as follows: LM6 (1:1, v/v), LM10 and LM11 (1:10, v/v; Plant Probes for both). The secondary antibody was a goat anti-rat IgG coupled to the fluorescent dye Alexa Fluor 633 (Molecular Probes) and was used at a 1:1,000 (v/v) dilution. Observations were carried out using a Leica DM RXA2 microscope with a TCS SP2 scanning confocal system. Acquisition settings, including laser power, photomultiplier gain, field of view (X,Y dimension), Z-step, and pixel size of the image, were strictly identical to ensure reliable comparisons between plant material (i.e. the wild type versus transformants or mutants). For each comparison, all sample preparation and observations were performed on the same day. For each experiment, three plants per line (the wild type, transformant, or mutant) and two sections per plant were observed. Three independent experiments for each comparison were performed.

In-Section ARAF Activity Assays

Resin-embedded lower parts of the stem sections (1 μm) were placed on Teflon-coated slides and blocked for 2 h at room temperature with PBST-BSA. Sections were washed with 200 mM acetate-Triton buffer (pH 4.0; 0.015% Triton X-100). Forty microliters of acetate-Triton buffer containing 120 microunits of enzyme were placed on the sections, and the reaction was carried out

for 5 d at 23°C. Every 24 h, the enzyme mixture was replaced with a fresh preparation. Sections were then washed with PBST and immunohistochemistry was carried out as indicated above, starting with the addition of the primary antibody. The enzymes used were an α-L-arabinofuranosidase from *Aspergillus niger* (Megazyme) and an Arabidopsis ARAF1 preparation obtained as described below. One unit is defined as the amount of enzyme required to hydrolyze 1 μmol min^{-1} pNPA in acetate buffer (200 mM, pH 4.0). Based on its molecular mass and pI, the *A. niger* enzyme belongs to the GH 51 CAZY family (Megazyme technical service).

ELISAs

Total protein extracts were prepared according to Harholt et al. (2006), and protein concentration was determined using the bicinchoninic acid method. Two micrograms of protein extract was then diluted 1:500 (v/v) in PBS to obtain a linear response throughout the protein concentration range used. Ninety-six-well microtiter plates were coated overnight at room temperature with increasing amounts of diluted protein extract. Unbound protein was washed with PBS, and plates were blocked with PBS, 0.1% (v/v) Tween 20, and 1% (w/v) BSA (PBST-BSA). LM6 antibody (50 μL) diluted 1:200 (v/v) in PBST-BSA was added and left for 2 h at room temperature. Unbound antibodies were washed, and 50 μL of alkaline phosphatase-linked anti-rat IgG antibody (Sigma) diluted 1:2,000 (v/v) in PBST-BSA was added and left for 1 h at room temperature. Unbound antibodies were washed, 100 μL of the pNPP Liquid Substrate System for ELISA (Sigma) was added, and the A_{405} was measured with an ELISA plate reader (Eflab).

Chromatographic Separation of α-L-Arabinofuranosidase Activities

ARAF1 enzyme activity in *araf1-1* mutant, wild-type, and *araf1-1* stems were analyzed. Crude protein extracts were separated by cation-exchange chromatography and tested for α-L-arabinofuranosidase activity as described by Minic et al. (2004). Briefly, 2 g of stem tissue was ground in 25 mM BisTris buffer (pH 7.0) containing 200 mM $CaCl_2$, 10% (v/v) glycerol, 4 μM sodium cacodylate, and Protease inhibitor cocktail (1:200, v/v; Sigma). Two milliliters (1.0 mg) of soluble protein extract was equilibrated in 25 mM acetate buffer (pH 5.0) containing 2% (v/v) glycerol and 0.015% (v/v) Triton X-100 and loaded on a CM-Sepharose (Sigma) cation-exchange column (1.5 cm × 4 cm). Proteins were eluted in the same buffer with a 0 to 0.4 M NaCl discontinuous gradient in steps of 2.5 mL per 0.025 M NaCl. One-milliliter fractions were collected, and 50 μL was assayed for α-L-arabinofuranosidase activity using pNPA as substrate, as described by Minic et al. (2004).

For in-section activity assays, ARAF1 enzyme from *35S::ARAF1b* stems was obtained by lectin chromatography followed by cation-exchange chromatography. Crude protein extract was bound in-batch to 1 mL of concanavalin A resin (Sigma) equilibrated in 20 mM Tris buffer (pH 7.4) containing 0.5 M NaCl. Resin was washed with 10 volumes of the same buffer and transferred to an empty 1-mL column. Protein was eluted in a single step with 2 mL of the same buffer containing 0.2 M methyl-α-D-glucopyranose. Eluted proteins were equilibrated and separated by cation-exchange chromatography as described above. The first arabinofuranosidase activity peak eluted from the cation-exchange column contained only one arabinofuranosidase activity, ARAF1. These fractions were pooled and stored at 4°C until use. The lectin chromatography step is necessary to remove the ARAF2 enzyme (Z. Minic and L. Jouanin, unpublished data).

Transcriptome Analysis

The microarray analysis was carried out using the CATMA (Crowe et al., 2003; Hilson et al., 2004), containing 24,576 gene-specific tags from Arabidopsis (Thareau et al., 2003). The spotting of the gene-specific tag amplicons on array slides and the array analysis process have been described by Lurin et al. (2004). RNA was extracted and pooled from the lower part of the stems of two different cultures of Ws, *araf1-1*, Col0, and *35S::ARAF1b* plants grown under the same exact environmental conditions. For each comparison, one technical replication with fluorochrome reversal was performed for each pool of RNA. RNA integrity, cDNA synthesis, hybridization, and array scanning were performed as described by Vergnolle et al. (2005). Statistical analysis was based on two dye swaps per comparison (Ws versus *araf1-1* and Col0 versus *35S::ARAF1b*). For each array, the raw data comprised the logarithm of median feature pixel intensity at wavelengths 635 nm (red) and 532 nm (green). No background was subtracted. In the following description, log ratio refers to the differential expression between the wild type and mutant or overexpressor. An array-by-array normalization was performed to remove systematic biases. First, we excluded spots that were considered to show badly formed features by the experimenter. Then, we performed a global intensity-dependent normalization using the LOESS procedure (Yang et al., 2002) to correct the dye bias. Finally, on each block of the array, the log ratio median was subtracted from each value of the log ratio of the block to correct any print tip effect on each block. To determine differentially expressed genes, we performed a paired *t* test on the log ratios, assuming that the variance of the log ratios is the same for all genes. Spots displaying extremes of variance (too small or too large) were excluded. The raw *P* values were adjusted by the Bonferroni method, which controls the family-wise error rate. We considered as differentially expressed the genes with a Bonferroni $P < 5\%$, as described by Lurin et al. (2004).

Sequence data from this article were deposited in the GEO database according to MIAME standards under accession numbers GSE7420 and GSE7421.

Supplemental Data

The following materials are available in the online version of this article.

Supplemental Table S1. Genes differentially expressed in the lower part of *araf1-1* stems.

Supplemental Table S2. Genes differentially expressed in the lower part of *35S::ARAF1b* stems.

ACKNOWLEDGMENTS

We thank Amandine Freydier for all her help during mutant screening; the John Innes Centre and Julie Cullimore for their kind gift of the pGreen plasmid; Jean-Louis Luc and Patricia Panegos for their invaluable help with Arabidopsis cultures; and Simon McQueen-Mason for stomatal function experiments. A special acknowledgment goes to Fabienne Guillon for her insightful discussions on anti-xylan antibody affinity.

Received September 28, 2007; accepted March 13, 2008; published March 14, 2008.

LITERATURE CITED

Aspeborg H, Schrader J, Coutinho PM, Stam M, Kallas A, Djerbi S, Nilsson P, Denman S, Amini B, Sterky F, et al (2005) Carbohydrate-active enzymes involved in the secondary cell wall biogenesis in hybrid aspen. Plant Physiol **137:** 983–997

Bauer S, Vasu P, Persson S, Mort AJ, Somerville CR (2006) Development and application of a suite of polysaccharide-degrading enzymes for analyzing plant cell walls. Proc Natl Acad Sci USA **103:** 11417–11422

Bechtold N, Ellis J, Pelletier G (1993) *In planta* Agrobacterium mediated gene transfer by infiltration of adult *Arabidopsis thaliana* plants. C R Acad Sci Paris Life Sci **316:** 1194–1199

Borkhardt B, Skjøt M, Mikkelsen R, Jørgensen B, Ulvskov P (2005) Expression of a fungal endo-[alpha]-1,5-l-arabinanase during stolon differentiation in potato inhibits tuber formation and results in accumulation of starch and tuber-specific transcripts in the stem. Plant Sci **169:** 872–881

Bouton S, Leboeuf E, Mouille G, Leydecker MT, Talbotec J, Granier F, Lahaye M, Höfte H, Truong HN (2002) *QUASIMODO1* encodes a putative membrane-bound glycosyltransferase required for normal pectin synthesis and cell adhesion in *Arabidopsis*. Plant Cell **14:** 2577–2590

Boyes DC, Zayed AM, Ascenzi R, McCaskill AJ, Hoffman NE, Davis KR, Görlach J (2001) Growth stage-based phenotypic analysis of *Arabidopsis*: a model for high throughput functional genomics in plants. Plant Cell **13:** 1499–1510

Burget EG, Reiter WD (1999) The *mur4* mutant of Arabidopsis is partially defective in the de novo synthesis of uridine diphospho L-arabinose. Plant Physiol **121:** 383–389

Burget EG, Verma R, Molhoj M, Reiter WD (2003) The biosynthesis of L-arabinose in plants: molecular cloning and characterization of a Golgi-

localized UDP-D-xylose 4-epimerase encoded by the *MUR4* gene of *Arabidopsis*. Plant Cell **15:** 523–531

Carafa A, Duckett JG, Knox JP, Ligrone R (2005) Distribution of cell-wall xylans in bryophytes and tracheophytes: new insights into basal interrelationships of land plants. New Phytol **168:** 231–240

Charmont S, Jamet E, Pont-Lezica R, Canut H (2005) Proteomic analysis of secreted proteins from *Arabidopsis thaliana* seedlings: improved recovery following removal of phenolic compounds. Phytochemistry **66:** 453–461

Clough SJ, Bent AF (1998) Floral dip: a simplified method for Agrobacterium-mediated transformation of *Arabidopsis thaliana*. Plant J **16:** 735–743

Coutinho PM, Henrissat B (1999) Carbohydrate-active enzymes: an integrated database approach. *In* HJ Gilbert, G Davies, B Henrissat, B Svensson, eds, Recent Advances in Carbohydrate Bioengineering. Royal Society of Chemistry, Cambridge, UK, pp 3–12

Crowe ML, Serizet C, Thareau V, Aubourg S, Rouze P, Hilson P, Beynon J, Weisbeek P, van Hummelen P, Reymond P, et al (2003) CATMA: a complete Arabidopsis GST database. Nucleic Acids Res **31:** 156–158

Demura T, Tashiro G, Horiguchi G, Kishimoto N, Kubo M, Matsuoka N, Minami A, Nagata-Hiwatashi M, Nakamura K, Okamura Y, et al (2002) Visualization by comprehensive microarray analysis of gene expression programs during transdifferentiation of mesophyll cells into xylem cells. Proc Natl Acad Sci USA **99:** 15794–15799

Dolezal O, Cobbett C (1991) Arabinose kinase-deficient mutant of *Arabidopsis thaliana*. Plant Physiol **96:** 1255–1260

Fulton LM, Cobbett CS (2003) Two alpha-L-arabinofuranosidase genes in *Arabidopsis thaliana* are differentially expressed during vegetative growth and flower development. J Exp Bot **54:** 2467–2477

Gibeaut D, Carpita N (1991) Tracing cell wall biogenesis in intact cells and plants: selective turnover and alteration of soluble and cell wall polysaccharides in grasses. Plant Physiol **97:** 551–561

Gomez LD, Baud S, Gilday A, Li Y, Graham IA (2006) Delayed embryo development in the Arabidopsis TREHALOSE-6-PHOSPHATE SYNTHASE 1 mutant is associated with altered cell wall structure, decreased cell division and starch accumulation. Plant J **46:** 69–84

Goujon T, Minic Z, El Amrani A, Lerouxel O, Aletti E, Lapierre C, Joseleau JP, Jouanin L (2003) *AtBXL1*, a novel higher plant (*Arabidopsis thaliana*) putative beta-xylosidase gene, is involved in secondary cell wall metabolism and plant development. Plant J **33:** 677–690

Harholt J, Jensen JK, Sorensen SO, Orfila C, Pauly M, Scheller HV (2006) ARABINAN DEFICIENT 1 is a putative arabinosyltransferase involved in biosynthesis of pectic arabinan in Arabidopsis. Plant Physiol **140:** 49–58

Hilson P, Allemeersch J, Altmann T, Aubourg S, Avon A, Beynon J, Bhalerao RP, Bitton F, Caboche M, Cannoot B, et al (2004) Versatile gene-specific sequence tags for Arabidopsis functional genomics: transcript profiling and reverse genetics applications. Genome Res **14:** 2176–2189

Jamet E, Canut H, Boudart G, Pont-Lezica RF (2006) Cell wall proteins: a new insight through proteomics. Trends Plant Sci **11:** 33–39

Jones L, Milne JL, Ashford D, McQueen-Mason SJ (2003) Cell wall arabinan is essential for guard cell function. Proc Natl Acad Sci USA **100:** 11783–11788

Koornneef M, Alonso-Blanco C, Peeters A, Soppe W (1998) Genetic control of flowering time in Arabidopsis. Annu Rev Plant Physiol Plant Mol Biol **49:** 345–370

Kotake T, Tsuchiya K, Aohara T, Konishi T, Kaneko S, Igarashi K, Samejima M, Tsumuraya Y (2006) An alpha-L-arabinofuranosidase/beta-D-xylosidase from immature seeds of radish (*Raphanus sativus* L.). J Exp Bot **57:** 2353–2362

Leboeuf E, Thoiron S, Lahaye M (2004) Physico-chemical characteristics of cell walls from *Arabidopsis thaliana* microcalli showing different adhesion strengths. J Exp Bot **55:** 2087–2097

Lee KJD, Sakata Y, Mau SL, Pettolino F, Bacic A, Quatrano RS, Knight CD, Knox JP (2005) Arabinogalactan proteins are required for apical cell extension in the moss *Physcomitrella patens*. Plant Cell **17:** 3051–3065

Lee RC, Burton RA, Hrmova M, Fincher GB (2001) Barley arabinoxylan arabinofuranohydrolases: purification, characterization and determination of primary structures from cDNA clones. Biochem J **356:** 181–189

Lee RC, Hrmova M, Burton RA, Lahnstein J, Fincher GB (2003) Bifunctional family 3 glycoside hydrolases from barley with alpha-L-arabinofuranosidase and beta-D-xylosidase activity: characterization, primary structures, and COOH-terminal processing. J Biol Chem **278:** 5377–5387

Lurin C, Andres C, Aubourg S, Bellaoui M, Bitton F, Bruyere C, Caboche M, Debast C, Gualberto J, Hoffmann B, et al (2004) Genome-wide analysis of *Arabidopsis* pentatricopeptide repeat proteins reveals their essential role in organelle biogenesis. Plant Cell **16:** 2089–2103

McCartney L, Marcus SE, Knox JP (2005) Monoclonal antibodies to plant cell wall xylans and arabinoxylans. J Histochem Cytochem **53:** 543–546

Milioni D, Sado PE, Stacey NJ, Domingo C, Roberts K, McCann MC (2001) Differential expression of cell-wall-related genes during the formation of tracheary elements in the Zinnia mesophyll cell system. Plant Mol Biol **47:** 221–238

Minic Z, Do CT, Rihouey C, Morin H, Lerouge P, Jouanin L (2006) Purification, functional characterization, cloning, and identification of mutants of a seed-specific arabinan hydrolase in Arabidopsis. J Exp Bot **57:** 2339–2351

Minic Z, Jamet E, Negroni L, Arsene der Garabedian P, Zivy M, Jouanin L (2007) A sub-proteome of *Arabidopsis thaliana* mature stems trapped on concanavalin A is enriched in cell wall glycoside hydrolases. J Exp Bot **58:** 2503–2512

Minic Z, Rihouey C, Do CT, Lerouge P, Jouanin L (2004) Purification and characterization of enzymes exhibiting beta-D-xylosidase activities in stem tissues of Arabidopsis. Plant Physiol **135:** 867–878

Pesquet E, Ranocha P, Legay S, Digonnet C, Barbier O, Pichon M, Goffner D (2005) Novel markers of xylogenesis in zinnia are differentially regulated by auxin and cytokinin. Plant Physiol **139:** 1821–1839

Rosso MG, Li Y, Strizhov N, Reiss B, Dekker K, Weisshaar B (2003) An *Arabidopsis thaliana* T-DNA mutagenized population (GABI-Kat) for flanking sequence tag-based reverse genetics. Plant Mol Biol **53:** 247–259

Saulnier L, Marot C, Chanliaud E, Thibault JF (1995) Cell wall polysaccharide interactions in maize bran. Carbohyrate Polymers **26:** 279–287

Schluepmann H, Pellny T, van Dijken A, Smeekens S, Paul M (2003) Trehalose 6-phosphate is indispensable for carbohydrate utilization and growth in *Arabidopsis thaliana*. Proc Natl Acad Sci USA **100:** 6849–6854

Schrader J, Nilsson J, Mellerowicz E, Berglund A, Nilsson P, Hertzberg M, Sandberg G (2004) A high-resolution transcript profile across the wood-forming meristem of poplar identifies potential regulators of cambial stem cell identity. Plant Cell **16:** 2278–2292

Skjøt M, Pauly M, Bush MS, Borkhardt B, McCann MC, Ulvskov P (2002) Direct interference with rhamnogalacturonan I biosynthesis in Golgi vesicles. Plant Physiol **129:** 95–102

Tateishi A, Mori H, Watari J, Nagashima K, Yamaki S, Inoue H (2005) Isolation, characterization, and cloning of {alpha}-L-arabinofuranosidase expressed during fruit ripening of Japanese pear. Plant Physiol **138:** 1653–1664

Thareau V, Dehais P, Serizet C, Hilson P, Rouze P, Aubourg S (2003) Automatic design of gene-specific sequence tags for genome-wide functional studies. Bioinformatics **19:** 2191–2198

Thibault JF (1979) Automatisation du dosage des substances pectiques par la methode au meta-hydroxydiphenyl. Lebensm Wiss U Technol **12:** 247–251

van Dijken AJH, Schluepmann H, Smeekens SCM (2004) Arabidopsis trehalose-6-phosphate synthase 1 is essential for normal vegetative growth and transition to flowering. Plant Physiol **135:** 969–977

Vergnolle C, Vaultier MN, Taconnat L, Renou JP, Kader JC, Zachowski A, Ruelland E (2005) The cold-induced early activation of phospholipase C and D pathways determines the response of two distinct clusters of genes in Arabidopsis cell suspensions. Plant Physiol **139:** 1217–1233

Willats WG, Marcus SE, Knox JP (1998) Generation of monoclonal antibody specific to (1→5)-alpha-L-arabinan. Carbohydr Res **308:** 149–152

Xiong J, Balland-Vanney M, Xie Z, Schultze M, Kondorosi A, Kondorosi E, Staehelin C (2007) Molecular cloning of a bifunctional {beta}-xylosidase/{alpha}-l-arabinosidase from alfalfa roots: heterologous expression in *Medicago truncatula* and substrate specificity of the purified enzyme. J Exp Bot **58:** 2799–2810

Yang YH, Dudoit S, Luu P, Lin DM, Peng V, Ngai J, Speed TP (2002) Normalization for cDNA microarray data: a robust composite method addressing single and multiple slide systematic variation. Nucleic Acids Res **30:** e15

Zhou GK, Zhong R, Richardson EA, Morrison WH III, Nairn CJ, Wood-Jones A, Ye ZH (2006) The poplar glycosyltransferase GT47C is functionally conserved with Arabidopsis Fragile fiber8. Plant Cell Physiol **47:** 1229–1240

Zimmermann P, Hirsch-Hoffmann M, Hennig L, Gruissem W (2004) GENEVESTIGATOR. Arabidopsis microarray database and analysis toolbox. Plant Physiol **136:** 2621–2632